Soft X-Ray Emission Spectra of Metallic Solids: Critical Review of Selected Systems

A. J. McAlister, R. C. Dobbyn, J. R. Cuthill, and M. L. Williams

Institute for Materials Research, National Bureau of Standards, Washington, D.C. 20234

Theory and experimental practice in the field of soft x-ray emission from metallic solids are briefly reviewed, and measurements on a number of systems (Al, Al in $AuAl_2$, Al and Mg in Al-Mg, Cu, Cu and Ni in Cu-Ni, Li, Mg, Na, and Ni) are critically evaluated and compared with the results of other techniques and theory, with a view to establishing the pertinence of the soft x-ray measurements and indicating specific guidelines for enhancing their value.

Key words: Alloys; critical review; emission spectra; intermetallic compounds; metals; soft x-ray; spectra.

1. Introduction

In recent years, considerable progress has been made in understanding the electronic structure of solids. On the theoretical side, within the framework of the independent particle model, the techniques of energy band theory have been developed to the extent that many experimenters are now employing them in the detailed interpretation of their own data. Ordered compounds as well as elemental materials are under investigation, and the theory of disordered systems is being actively pursued. In addition, the theory of many-body systems has progressed to the point that the general validity and limits of the independent particle approach are fairly well understood. Experimental progress has been no less dramatic. An impressive array of experimental techniques has been brought to bear on the problem. These techniques fall into two categories: Fermi level probes of metallic solids, such as the many techniques for gauging the Fermi surface, low temperature specific heat, the Knight shift; and broad probes of the electronic structure such as optical, photoemission, soft x-ray, ion neutralization, positron annihilation, and Compton spectroscopies. All of these techniques are being applied, with ever increasing refinement, to more and more systems. The obvious price of such progress is an enormous growth of the literature and the attendant danger of individual workers losing touch even with work in their own fields. Topical reviews are much needed to ward off this danger.

The present paper is intended to fulfill a part of this need by providing a selective critical review of one major aspect of one experimental technique. The technique is soft x-ray emission spectroscopy (SXS), a broad probe which explores the entire occupied band structure. We further restrict outselves to metals, in their pure state, in alloys, and in intermetallic compounds. We use the term "soft x-ray" in a special way. "X-ray" has its traditional sense of describing radiative transitions involving initial ion core level vacancies. But the term "soft" shall imply that the final vacancy lies within the conduction band. Thus, as illustrated in figure 1, the technique consists of producing vacancies in ion core levels, and observing the spontaneous radiation emitted when electrons initially in the conduction band drop into the vacant core states. Generally, photons emitted in this process are "soft" in the usual sense of being readily absorbed by the atmosphere, and measurements are of necessity carried out in vacuum instruments. This is not always the case however. The penetrating radiation emitted in conduction band to K level transitions in the $3d$ metals is "soft" by our definition. To further orient

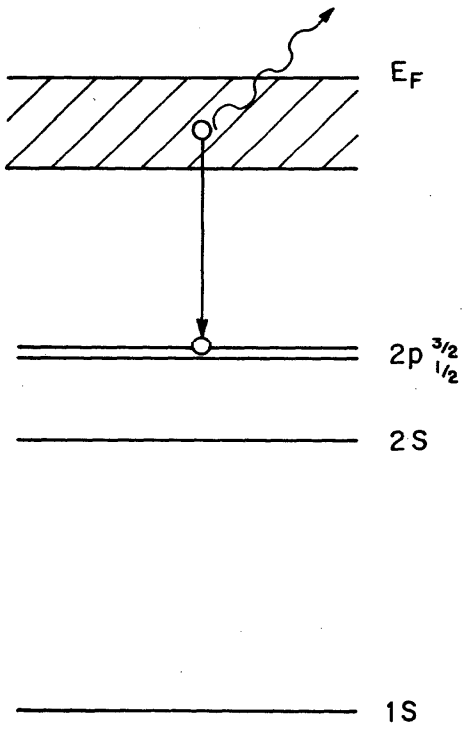

FIGURE 1. An energy level scheme, appropriate to Al metal, illustrating the soft x-ray emission process.

A vacancy of well defined energy is produced in some ion core level, by electron beam bombardment or photoemission. An electron from the conduction band may drop into the core hole, the relaxation being accompanied by emission of a soft x-ray photon. The energy distribution of the emitted photons reflects the distribution in energy in the conduction band of the particular orbital character allowed by the dipole selection rules.

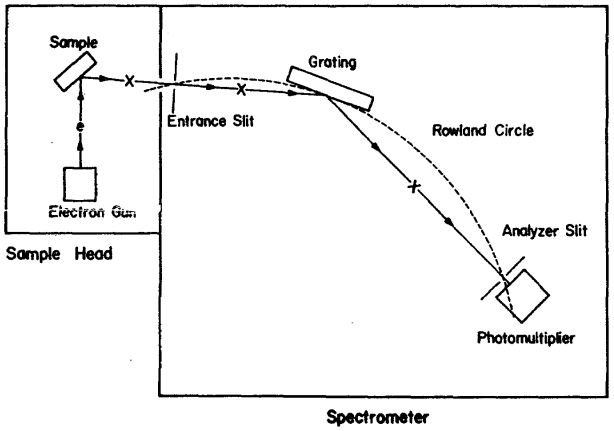

FIGURE 2. Layout of a typical soft x-ray system.

Any soft x-ray system must consist of (1) a sample head in which the x-rays are produced and (2) a spectrometer in which they are energy analyzed and detected. In most practical applications, each must be mounted in vacuum since the radiation is usually easily absorbed by the atmosphere. Where the radiation is highly penetrating, it is well to keep the sample head under vacuum, in the interest of sample cleanliness.

the reader unfamiliar with the field, a typical instrument is illustrated in figure 2. It consists of two major components: a sample head in which the soft x-rays are generated, and a spectrometer in which they are energy analyzed and detected. To achieve sample cleanliness and reliable, reproducible results, the sample should always be mounted in vacuum. If, as in the case illustrated, initial state ion core vacancies are prepared by electron bombardment, a vacuum system must be employed. If inner level vacancies are produced by photoemission (shining x-rays from a separate tube onto the sample, say) and penetrating radiation is produced, then the sample could be mounted in atmosphere, save for the reasons of cleanliness and reliability cited above. Figure 2 shows a particular type of spectrometer using a concave grating as the dispersing element and a driven photomultiplier as a detector. Other arrangements may be used, depending on spectral range and purpose. For instance, bent crystals and double crystals are used as dispersing elements in regions of higher photon energy. Proportional counters or photographic plates may be used as detectors as the application demands.

The specific objectives of this work are to promote better experimental practice and to afford theorists a better understanding of the problems and limitations of the measurements through critical analysis of a representative sampling of systems upon which two or more measurements have been performed. The theoretical basis for interpretation is outlined in section 2. Criteria for critical evaluation are developed in section 3 and summarized in the introduction to section 4. Critical evaluations are given in section 4 where, in addition to comparisons among soft x-ray measurements, comparison with theory and the results of other deep probe techniques is carried out as well. Since photoemission (X-ray, XPS, and ultraviolet, UPS) and ion neutralization (INS) will be the other techniques most frequently compared, a brief description of these techniques has been provided by figure 3.

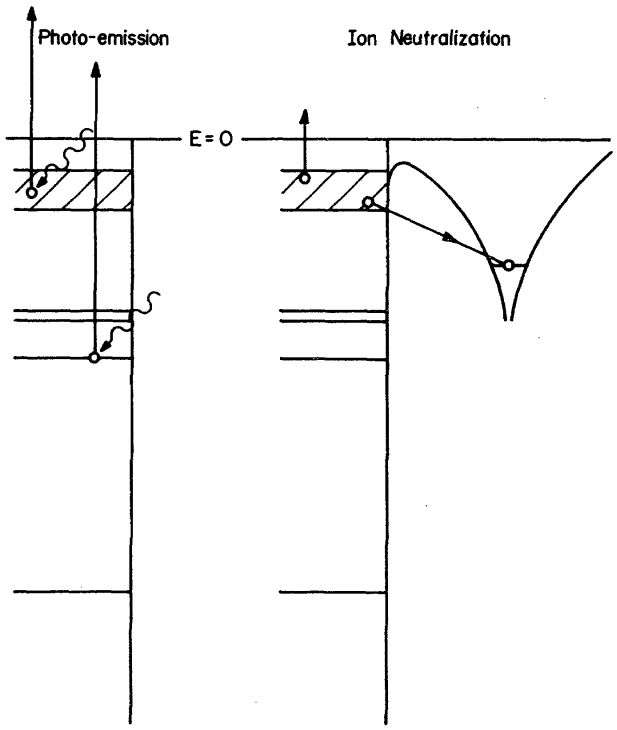

FIGURE 3. Comparison of photoemission and ion neutralization processes.

Photoemission (x-ray or uv induced): An incoming mono-energetic photon beam ejects electrons from the metal. If uv photons are used, only conduction band states are accessible for study; if x-rays are used, core states may be studied as well. The kinetic energy spectrum of ejected electrons yields information on the fold of occupied and unoccupied states. The two may be sorted out by varying the exciting photon beam energy. Ion neutralization: A low energy beam of noble gas ions impinges on the metal surface. If a vacant ion state lies below the conduction band of the metal, an Auger relaxation may occur at the surface, one electron of the Auger pair filling the ion vacancy, and the other being raised to an excited state whence it may escape the metal. The energy spectrum of ejected electrons contains information on the state density, though probably only near the surface.

2. Theoretical Situation

Conduction band emission spectroscopy is carried out by preparing vacancies in ion core levels, in the manner outlined in the previous section, then observing the energy distribution of photons spontaneously emitted as electrons initially in conduction band states drop into vacant core levels. Since the core levels are relatively sharp, some picture of the energy distribution of the conduction band states is expected to emerge. To proceed further, we note that the core states are localized, normally occupying much less than a unit cell volume. Furthermore, in typical experiments, the density of ions with vacant core levels is low enough that the probability of their interacting is negligible. Thus the dimensions of the radiating system are small compared to a wavelength, and the dipole approximation is valid. One can then write for the photon emission rate

$$R(\omega) \propto \omega/l \sum_{i,f} |<\psi_f| \sum_k \vec{p}_k |\psi_i>|^2 \, \delta(h\omega - E_i + E_f)$$

where $\vec{p}$ is electron momentum. The k sum ranges over all electrons of the system, the i sum over l initial states, and the f sum over all final states. ψ_i and ψ_f are exact state vectors; E_i and E_f their energies. The usual dipole selection rules apply, and thus the emitted spectrum depends on the orbital symmetry of the inner level: a K level samples only the p-orbital admixture of the conduction band; L_2 and L_3 levels the s and d orbital admixture.

The above expression for the soft x-ray emission spectrum is exact so far as the crystalline states are concerned. It can be solved in several approximations, in the simplest of which dynamic interactions between the electrons and local charge reorganization due to the presence of the core hole are ignored. ψ_i and ψ_f are approximated by antisymmetric linear combinations of single particle wave functions, ψ_i describing N conduction states plus a core with a vacancy, ψ_f an excited state containing $N-1$ conduction states and a full core. If the initial and final states are represented by linear combinations constructed from the same orthonormal set, the matrix element reduces to a sum of terms involving only single initial core and final band states. In the first attempt at this sort of analysis, Houston [1][1] used free electron wave functions for the conduction band states, an approach which ignores the fact that the strongly localized core functions sample the band states near the nucleus where free electron waves form a very poor approximation to the Bloch states. This factor, and an approximate accounting of the effect of crystal symmetry on the orbital admixture of the band states, were introduced by Jones, Mott, and Skinner [2]. Only recently have attempts been made to carry this one electron approach further by detailed calculations based on band theoretical results. While only a few systems have as yet been studied in this way—pure Al and Cu, Al in $AuAl_2$, all discussed in some detail in section 4 below—*structural* agreement with experiment is remarkably good.

A number of features of the observed emission profiles cannot be explained by the one-electron model described above. Broad low energy tails and weak satellites on the low energy side, shifted down from the main band by the plasmon energy are obvious examples. Moreover, while structural features such as peaks and edges occur at predicted locations, their observed amplitudes and sharpness differ from the simple one electron prediction, and seem to require screening and lifetime effects for their explanation. A number of workers have examined the effects of charge reorganization about the core hole in the one electron approximation—Friedel [3], Goodings [4], Allotey [5]—emphasizing light metal spectra, particularly the Li K spectrum (Tomboulian and Bedo [6]), which displays a puzzling early peak, about 0.6 eV below the high energy edge. It seems fair to say that their results, while plausible, offer no definitive explanation of the observed profiles. See particularly the discussion of the Li K spectrum given below. The first attempt to account for the effects of the electron-electron interaction (beyond the usual effective potential of the one electron approach) was carried out by Landsberg [7], who used a static screened interaction to compute the energy dependent lifetime of final state conduction band holes. In this way, he was able to account for the broad low energy tail of the Na $L_{2,3}$ spectrum. Despite the rather good fit obtained, this result was defective in several respects. Since a static interaction was used, the method could not handle the plasmon satellite (observed later; see Rooke [8]). The small pip seen at the high energy edge (Skinner [9] and later work discussed below) remained unexplained. Landsberg adjusted the screening length to give best fit. The length giving optimum fit was significantly shorter than that computed from Bohm-Pines [10] theory. This situation worsened when Pirenne and Longe [11] introduced the further effect of electrons virtually scattered from the core defect. Energy must be supplied to make the virtual processes real when a photon is emitted, and further broadening is introduced. The static screening length needed to fit experiment when this process is introduced results in further deviation from the Bohm-Pines length. A successful resolution of the plasmon and screening length difficulties was given by Glick and Longe [12], who calculated the intensity of the tailing including the plasmon satellite, of the Na $L_{2,3}$ spectrum by carrying out a many body perturbation estimate of the matrix elements, including only the lowest order terms contributing to the tail region. The earlier discrepancy with Bohm-Pines theory was found to have resulted from omission of certain cross terms in the static approximation. The Glick-Longe first order theory, however, diverged in the main band. Together with Bose [13], they extended the work to the main band by summing over certain classes of terms in the many body expansion. A notable result of this latter work was a distinct enhancement of intensity at the high energy edge, resulting from a heavy production of virtual electron-hole pairs via dynamic scattering from the core hole. This provides a natural explanation for the emission edge pip observed in the Na spectrum, and agrees well with the independent analyses of the effects of sudden decay (or build up) of screening charge about the ion core defect upon emission (or absorption) edge intensities by Mahan [14] and Nozieres and de Dominicis [15]. Particular attention should be called to the work of Hedin and Lundqvist [16], whose work on the relation between structural peaks in the spectral distribution function of the interacting electron gas, the eigen-energies of one electron theory, and the results of a variety of experiments including soft x-ray emission spectroscopy provides the most convincing theoretical rationalization of the agreement cited above between one electron estimates of soft x-ray profiles and experiment.

[1] Numbers in brackets indicate references at the end of this paper.

3. Remarks on Experimental Practice

It is not out purpose here to discuss instrumental details and technique. The interested reader will find much useful information and many references in Parratt's classic review [17], the Strathclyde Conference proceedings, edited by Fabian [18], and the recent text by Samson [19]. Rather, we focus attention on those aspects of current experimental practice which most directly affect interpretation of emission band spectra. In this connection it is important to note that the true emission spectrum is not measured, but rather the quantity

$$R_m(\omega_s) = \int_{-\infty}^{\infty} d\omega R(\omega) S(\omega) \rho(\omega) W(\omega - \omega_s)$$

where R_m is the measured emission rate at frequency setting ω_s, $R(\omega)$ the true emission spectrum at frequency ω, $S(\omega)$ the fraction of emitted photons escaping the sample (self absorption factor), $\rho(\omega)$ the probability of a photon of energy $\hbar\omega$ being detected, and $W(\omega - \omega_s)$ the instrumental window function. The true emission rate $R(\omega)$ may not be (in fact, probably is never) the precise quantity theory would predict and experiment determine. Bulk or surface contaminants could well contribute a spurious component. More typically, overlapping contributions may arise when several initial states not widely separated in energy occur. Thus, for instance, the measured L profile of Al inevitably consists of strongly overlapping L_2 and L_3 profiles, accompanied by a negligibly weak partially overlapping high energy satellite as well (Neddermeyer and Wiech [20]). These problems are more pronounced in the M spectra of Cu and Ni, and are discussed in the following section. They can be dealt with in some cases, but their existence and the problems involved in correcting data for their presence should be born in mind by the reader, and stressed by the experimenter in reporting his results.

A number of advances have been made in experimental technique over the last decade. The use of improved vacuum technique lends greater confidence in the more current results. Two other advances are perhaps more significant. The introduction of photon counting techniques and digital recording systems has resulted in accurately linear response and known statistical confidence levels. Such work as Rooke's study of the plasmon satellites of the light metals [8] and the identification of 3*d*-band structural features in the M_3 emission spectra of Cu (Dobbyn, et al. [21]) and Ni (Cuthill, et al. [22]) would not have been possible without this technique. Equally important is the growing realization of the effects of self absorption on emission profiles. In this regard, Bonnelle [23] demonstrated the utility of optimizing x-ray takeoff and exciting electron beam incidence angles. Liefeld [24, 25] has demonstrated that the many discrepancies among recorded 3*d*-metal L_3 emission profiles arose mainly from differences in satellite and self absorption weightings due to differences in excitation conditions. It is of interest to note that the threshold effects observed in available Na L and Li K emission spectra (see the discussion in the next section), so important to the verification of current theory, may be affected to a significant degree by self absorption. Of course, when excitation conditions are accurately known, and in addition, the absorption coefficient of the sample is known over the appropriate spectral range (the latter is not usually the case), self absorbed spectra can be theoretically corrected. (See for instance, Yakowitz and Heinrich [26].)

Systematic uncertainties still remain a problem in the field. (See for instance the discussion of Al profiles in the following section.) We address ourselves here, if not to their complete elimination, at least to the suggestion that measurements to be reported in sufficient detail that their importance can be assessed by the reader. The major reasons for this problem are evidently the unique character of each instrument in use, and the lack of any standard instrumental comparison technique. The major difficulties appear to be as follows. The frequency response $\rho(\Omega)$ of dispersing elements and detectors is seldom known. Measurements on the same material are often made under different excitation conditions; not only does the intensity of excitation vary (exciting voltage and current density, say, in the case of electronic excitation), but the excitation geometry (exciting beam incidence and x-ray takeoff angles) usually differs as well. Hence $S(\omega)$ and satellite contributions to $R(\omega)$ can vary from measurement to measurement. Removal of background from electronically excited spectra is complicated by all of these factors. And too often, statements of slit settings and estimates of the inherent, varying instrumental resolution, $W(\omega - \omega_s)$ (the spectral window) are omitted, not surprisingly in the case of grating instruments, where no simple experimental method of estimating W is available. These problems are not insuperable, of course, but in most cases their complete solution involves considerable difficulty. When painstaking efforts have been made to assess the instrumental response, as in the work of Neddermeyer and Wiech on Al [20] and Neddermeyer on Mg [27], then a detailed report of spectra measured on the calibrated instrument should serve as a valuable secondary calibration standard. However, the low L_2/L_3 intensity ratios observed in these measurements indicate that they have been made at low x-ray takeoff and high electron incidence angles. The authors do not give these numbers. (They can be found in Neddermeyer's thesis [28]; however, they are not cited in the published papers.) Now one must either reproduce their excitation conditions, or, knowing the appropriate absorption coefficients, correct for differences in excitation conditions when using their data for calibration. Thus the utility of their results as a secondary calibration standard is limited, not by the presence of self-absorption in the

profile, but by the authors' omission of a conveniently accessible complete summary of the conditions under which the measurements were made.

Other examples could be cited, but these few seem sufficient basis for recommending that the following guidelines be followed by all workers in reporting emission spectra. This information should be given or some *readily accessible* source cited in all papers.

A. *The Instrument*
- (i) Method of calibration.
- (ii) Estimates of frequency response. If no estimate is made, give type and nature of dispersing element, settings.
- (iii) Report of resolution tests.
- (iv) Type of detector and recording system.

B. *Excitation*
- (i) Type: x-ray or electron. Monochromaticity. Current density and voltage.
- (ii) Geometry: beam incidence and x-ray takeoff angles.

C. *Sample*
- (i) Preparation: purity of starting materials, method.
- (ii) Characterization: type of tests and results. *Particularly important for alloys and compounds.*
- (iii) Handling. Before mounting; in vacuum before and during measurements. Tests made in instrument (e.g. scans for C and O K emission bands).

D. *Data Treatment*
- (i) Explain everything clearly—all corrections, smoothings, unfoldings.
- (ii) Show raw measured data, indicating statistical confidence level.

4. Critical Survey of Selected Main Band Results

In the following critical survey, we deal with complete transcribed spectral profiles rather than such commonly used spectroscopic parameters as peak position, half-width, and asymmetry index. We do so because spectroscopic parmeters can be strongly affected by the experimental problems cited above, and because it is the existence or otherwise of characteristic structure in the profiles, rather than coarse general features, which is of most interest to the student of electronic structure. Only main bands will be presented. Unless otherwise indicated the ordinate is [Rate ($h\nu$) per unit energy]/ν^3, as given by the author or so adjusted. The abscissa is $E-E_F$ in eV, where E_F is the estimated position of the Fermi level. All curves are normalized at peak ordinate value. This is not the best choice in all cases; in some, it will in fact overemphasize discrepancies. Additionally, the curves are corrected for background, usually by the author, but by us using a simple linear approximation if he has not done so. All alloy concentrations are given in atomic percent.

The criteria for value judgements between measured profiles are those established in section 3. An ideal measurement will have been made on a clean, well characterized sample in an instrument with accurate energy calibration, known frequency response, and a sharp, known spectral window. Electromagnetic detection (i.e., photomultipliers or proportional counters) will have been used, and data of known statistical confidence level presented. Excitation conditions will have been clearly stated, and self absorption effects will be, if not eliminated, of readily assessible extent. In cases where many measurements have been made, we select for display those few which come closest to the ideal. (An occasional measurement, in particularly close agreement with one of those displayed, will be omitted for the sake of clarity in the figures; such an omission will be noted in the text). Where only two or three measurements are available, we show all which are free of obvious catastrophic error.

Al

In figure 4 are presented a number of results, experimental and theoretical, on the $L_{2,3}$ and K emission bands of metallic Al, the material most frequently studied by soft x-ray spectroscopists, as well as the photoemission spectrum recorded by Wooten, et al. [29] at $h\nu=11.3$ eV.

The $L_{2,3}$ measurements are from *a*) Formichev [30], *b*) Neddermeyer and Wiech [20, 28], *c*) Rooke [31]. All used electromagnetic detection. *b* presents an average of strip chart records; *a* total counts, accumulated point by point; *c* total counts, accumulated by summing many digitally recorded continuous sweeps of the spectrum. *a* and *b* used Au coated, blazed gratings, and have made measurements of and corrected for grating frequency response. *c* used an unblazed glass grating, and did not make response measurements; however he argues that his response is smooth and relatively flat. No sample temperatures were reported; *a* notes use of a water cooled anode. The curves have been shifted slightly to coincide at $Y=0.6$ on the leading edge (a Fermi energy estimate suggested by calculations cited below). All three are electronically excited. All appear to be rather strongly self absorbed at the edge. *a* and *b* have achieved better resolution than *c*, and their profiles are more intense at the band edge. Normalization to peak intensity therefore makes their curves appear weaker in the lower reaches of the emission band. The definition of the $L_{2,3}$ edges in *a* and *b* suggests that about the same resolution was achieved. In light of their attempts at determining instrumental frequency response, the discrepancies between *a* and *b* are puzzling. In any case, all three spectra show the same type of structure, as do the available band theo-

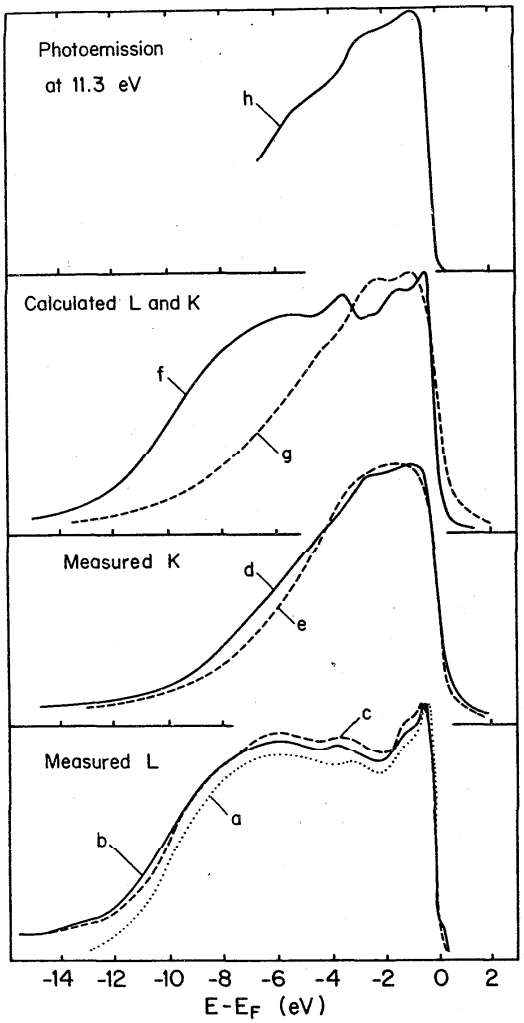

FIGURE 4. Aluminum.

Measured $L_{2,3}$ spectra, *a*–*c*; measured K-spectra, *d* and *e*; calculated L, *f*; calculated K, *g*; measured ultra violet photoemission spectrum at $h\nu = 11.3$ eV, *h*.

retical estimates of the profile (Rooke [32], Smrcka [33], and McAlister [34]). Other measurements showing the same structure have been reported: Sagawa [35]; Appleton and Curry [36]; Dimond [37] (the latter in very close agreement with *c*). Earlier work, in various respects less satisfactory than those cited above, by Catterall and Trotter [38], Skinner [9], and Cady and Tomboulian [39], is in essential agreement. Discrepancies certainly exist among the various measurements of the $L_{2,3}$ spectral profile. Their source is not clear. Temperature differences could play a role. The exact location of the deeper lying structure is liable to uncertainty from inherent noise, mode of data presentation, variations in instrumental response, and errors in estimating spectral dispersion. It seems safe to conclude, however, from the weight of experimental evidence, that the structure observed is real, though not at present perfectly characterized; and from the calculations, that it arises from band structure effects. Neither the calculations nor the measurements are sufficiently refined at present to ascertain the need for invoking singular edge behavior.

The two K profiles are from *d*) Deslattes [40] and *e*) Sénémaud [41]. *d* used a two crystal spectrometer and digital, stepwise recording of the output of an electromagnetic detector. *e* used a bent crystal instrument, and photographic recording and employed photorather than electron beam excitation. The results of *e* therefore needed no background correction. The overall shapes of the spectra are in good accord, particularly in view of our rough background correction [40] to *d*'s results. The results of *d* show weak, but clear structural features, which are in quite good agrement with the calculated result, curve g of figure 4. The failure of *e* (and other experimenters as well) to observe the structure in the K spectrum is in all likelihood due to the use of photographic detection (with only marginal response linearity) and the somewhat poorer resolution of the spectrometers employed.

The calculated profiles of McAlister [34] are shown here, the L-profile labelled *f*, and the K-profile labelled *g*. Of the three available estimates, we believe this one to have determined the orbital character of the band wave-functions most accurately. As noted above, the evident structural correlation between the calculated and measured profiles strongly suggests that band structure effects are being observed. The further structural correlation with the ultraviolet photoemission spectrum, curve *h* of figure 4, lends additional weight to this suggestion.

Al in $AuAl_2$

The measured $L_{2,3}$ profiles of Al from $AuAl_2$ shown in figure 5 are from *a*) Williams, et al. [42] and *b*) Curry and

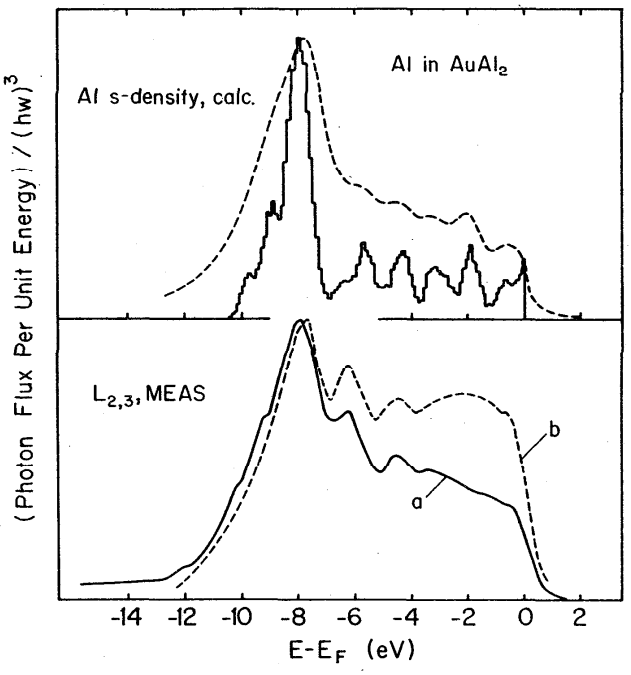

FIGURE 5. Aluminum in $AuAl_2$.

Lower curves, *a* and *b*, measured Al $L_{2,3}$ spectra from $AuAl_2$. Upper solid curve, calculated *s*-like state density at Al sites. Upper dashed curve *s*-like state density at Al sites subjected to a Landsberg smear.

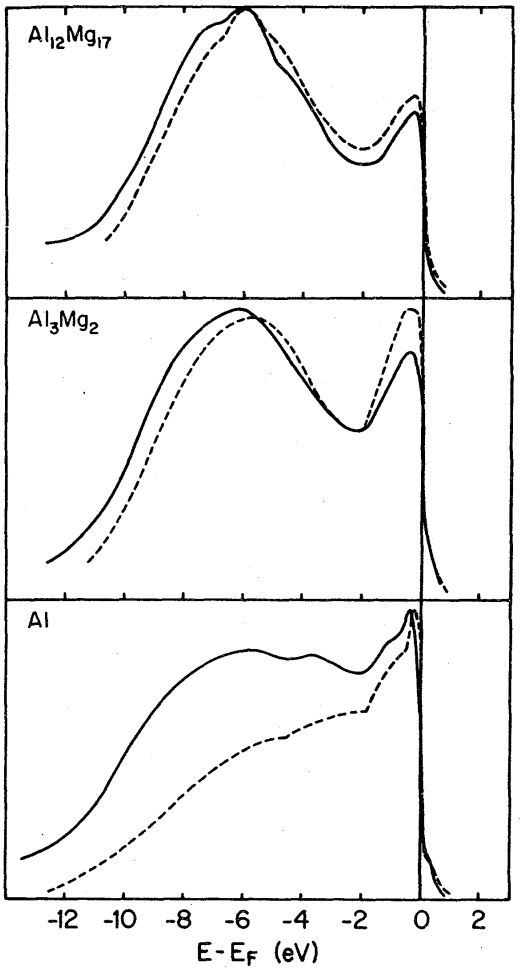

FIGURE 6. Aluminum in Al-Mg.

Measured Al $L_{2,3}$ emission spectra from Al and two Al-Mg compounds.

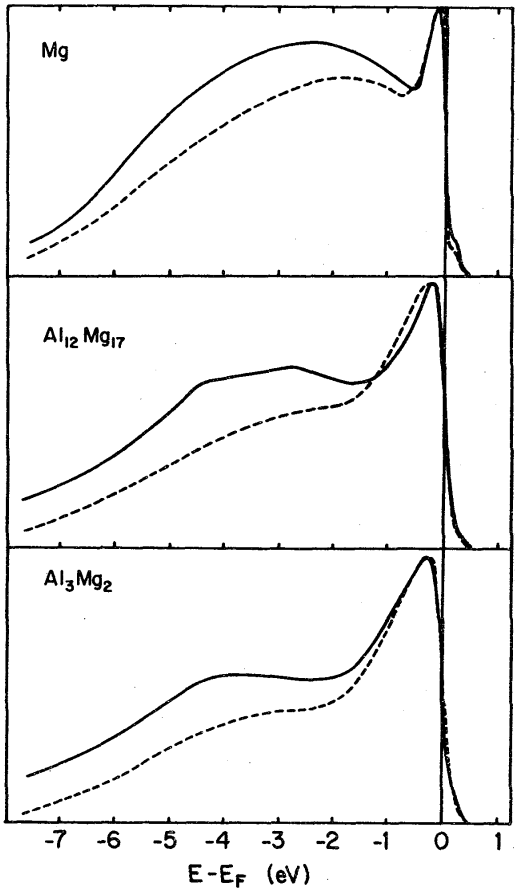

FIGURE 7. Magnesium in Al-Mg.

Measured Mg $L_{2,3}$ emission spectra from Mg and two Al-Mg compounds.

Harrison [43]. *a* used photoelectric detection, and summed many scans of the spectrum. *b* averaged several photographic records. The structural agreement between the two spectra is quite good. Comparison of $L_{2,3}$ spectra of pure Al from the two groups with other results (see above, and Appleton and Curry [36]) suggests that the overall difference between the profiles is due to spectrometer frequency response, the results of *b* being more severely affected. *a* appears to have achieved more nearly linear intensity response, and spent greater effort on specimen characterization. The upper curves of figure 5 give some theoretical estimate of the Al $L_{2,3}$ profile from the compound. The solid curve is Switendick's [44] estimate of the density of *s*-like states at Al sites. This has been shown (Goodings and Harris [45]; Bennett, et al. [46]; Dobbyn, et al. [21]) to be the leading term in a band theoretical estimate of the profile. The dashed curve is the result of applying an approximate Landsberg fold [7] to the Al *s*-density. The agreement seen between the calculation and the measured profiles is quite striking, as good in fact as that noted between measured and calculated pure Al $L_{2,3}$ spectra above.

Al and Mg in Al-Mg

In figures 6 and 7 are compared Al (fig. 6) and Mg (fig. 7) $L_{2,3}$ emission spectra from the pure metals and the compounds Al_3Mg_2 and $Al_{12}Mg_{17}$. The data are from *a*) Neddermeyer [27], solid curves, and *b*) Appleton and Curry [36], dashed curves. Both used electron beam excitation, *a* at 2.0 keV, *b* at 3.5 keV. Neither reported electron impingement or x-ray takeoff angles. No temperatures were reported, although *b* used water cooled targets. Stated pressures were: *a*, 4×10^{-8} and *b*, 1×10^{-6} torr. *a* used photoelectric detection, averaged several strip chart recordings of ratemeter output, and corrected his results for the known frequency response of his Au coated, blazed grating (Neddermeyer [28]). *b* used an unblazed glass grating, with photographic detection. As noted above (Al in $AuAl_2$), and evident here, *b*'s instrumental response increases markedly with photon energy, while *a*'s, on account of the quantum efficiency of the photocathode used (see Samson [19]) probably decreases slightly. Both *a* and *b* note that their compound samples probably deviate from stoichiometry by one or two percent.

Apart from the noted difference in instrumental frequency response, these two sets of measurements

are in good general agreement. Specific points of disagreement occur in the placement of the minimum of the pure Mg spectrum; the lack of structure in *b*'s Mg profile from $Al_{12}Mg_{17}$; and finally, in the shape of the Mg profiles from both of the compounds below −4.5 eV. In this energy range, *a*'s curves are noticeably concave, while *b*'s are slightly convex. This latter point is pertinent to understanding the electronic structure of this alloy system and needs further experimental clarification. Early measurements by Farineau [47] of the Al and Mg K-spectra from Al-Mg alloys showed equal experimental band widths for Al and Mg in the alloys, with the common width varying smoothly from that of pure Al to that of pure Mg across the system. More recent K measurements by Fischer and Baun [48] made under cleaner vacuum conditions, are in essential agreement with Farineau's work. (The validity of these K measurements is questionable, however, since strong self absorption effects may mask the true behavior. Re-investigation of the K spectra with this difficulty in mind would be of considerable interest.) The L spectra clearly behave in a radically different way, each component retaining essentially the same observed bandwidth throughout the composition range. This behavior is clearly shown in figure 8, where *a*'s Mg and Al spectra are overlaid. The compound data of figures 6 and 7 are repeated here, and additionally, results from a solid solution of 5 percent Al in Mg are shown. The latter sample was believed to be single phase. The striking difference in measured bandwidths seen here probably stems from the necessity of local charge neutrality in a metallic system. More charge must accumulate in regions of greatest potential, here at Al sites. Screening is evidently accomplished by states lowest in energy being heavily localized at Al sites, and perhaps being of different orbital symmetry there than at Mg sites. (This latter point is suggested by the concavity of the Mg $L_{2,3}$ from Al_3Mg_2 and $Al_{12}Mg_{17}$ below −4 eV. Normally, one anticipates convexity for L spectra in this energy range, owing to dominantly *s*-like local wave function character there. See Jones, et al. [2].) Direct substantiation of this picture by band computations for the compounds is ruled out at present because of their complicated crystal structure. However, a rough model computation by Jacobs [49] suggests that it is correct. Computational evidence does exist for energy dependent charging in other alloy systems. For instance, consider the calculations for $AuAl_2$ by Switendick [44] cited above, where Bloch functions of dominantly *d*-like character at Au sites are highly localised there, and exert influence on the charge distribution at Al sites largely through hybridization effects.

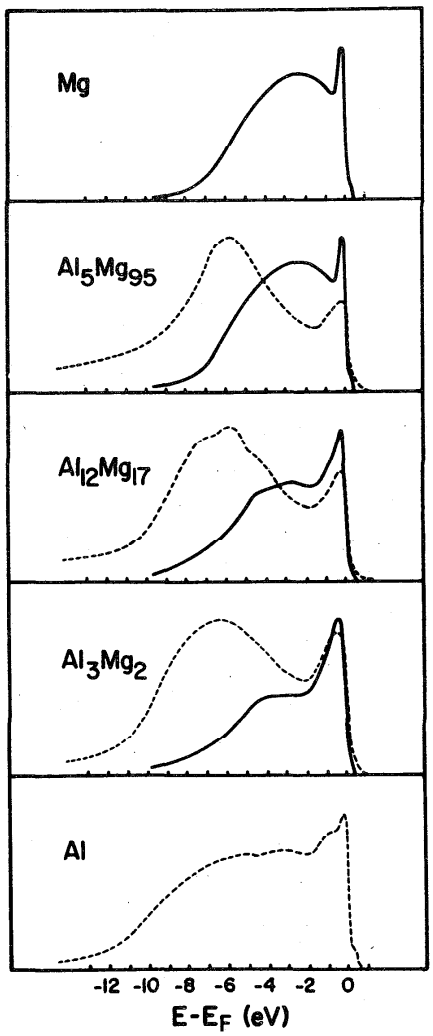

FIGURE 8. Aluminum and magnesium in Al-Mg.

Measured Al and Mg spectra, matched in energy at the Fermi edge and overlaid. Spectra from pure metals, the compounds Al_3Mg_2 and $Al_{12}Mg_{17}$, and the solid solution 5 percent Al in Mg.

Cu

In figure 9, 3 measurements of the Cu $M_{2,3}$ spectral complex are shown. These are smoothed, background corrected spectra, as presented by the authors save for a reduction of the data to a common plot of intensity (energy flux per unit energy) vs. photon energy. The

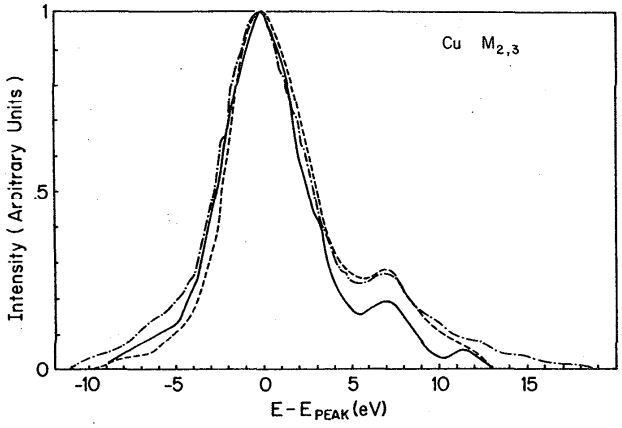

FIGURE 9. Copper.

Comparison of three measurements of the Cu $M_{2,3}$ emission spectrum, taken with different exciting electron beam voltages and different detection methods.

curves have been shifted by slight amounts (no more than 0.3 eV) to match in energy at peak intensity. They are otherwise faithful transcriptions of the published curves. These data are from *a*) Bedo and Tomboulian [50], solid curve; *b*) Dobbyn, et al. [21], dash-dot curve; and *c*) Clift, et al. [51], dashed curve. *a* and *c* used photographic detection; *b* photoelectric detection. *b* summed many digitally recorded scans of the spectrum, and in view of the linear response of photoelectric detection and the known standard counting error in their data (1.1 to 0.7%), assert the fine structure they observe to be reliably established. *a* and *c* report pressures of 1×10^{-6} torr, and used water cooled targets. *b* reported a pressure of 7×10^{-8} torr, with the target at 580° C well above the O_2 surface cleanup temperature of 277° C (Roberts [52]). All used electron beam excitation, with beam energies *a*) 1.5, *b*) 2.5, and *c*) 3.5 keV. The grazing angles of electron beam incidence were 90°, 20°, and 90°; x-ray take-off angles 45°, 90°, and 32° for *a*, *b*, and *c*, respectively. None attempted to assess self absorption effects. *a* and *b* identify the structure above 5 eV in figure 9 as satellites, *b* noting from energetic arguments they are likely to be double ionization satellites with the spectator hole residing in the M shell. This identification is supported by the trend in intensity of this structure relative to the main peak with exciting voltage. *b* (private communication) noted this same trend, comparing measurements made at 1.5 and 2.5 keV in the same instrument. *b* also noted that additional satellites, nearer the parent bands, are expected, with the spectator hole residing in the valence band. By treating the valence band satellites in a manner suggested by analysis of Liefeld's [24] measurements of the L_3 spectra of Cu and Ni at and above the L_2 threshold excitation voltage, and the M shell satellites in the intermediate coupling approximation, *b* argued that the major features of the Cu $M_{2,3}$ spectrum could be approximated by

$$M_{2,3}(E) = [M_3(E) + \alpha_1 M_3(E-\epsilon) + \alpha_2 M_3(E-2\epsilon)] + [\beta_1 M_3(E-\delta-2\epsilon/3) + \beta_2(E-\delta+\epsilon/\sqrt{3}) + \beta_3 M_3(E-\delta+2\epsilon/3)]$$

where $M_{2,3}(E)$ is the measured spectral complex and $M_3(E)$ the true single hole M_3 emission profile. The second bracketed term on the right approximates the satellites with the spectator hole residing in the $3p$ shell; the first represents the M_3 and M_2 parents and the satellites with spectator hole in the valence band. *b* inverted this expression and varied ϵ, the α's, and the β's over reasonable ranges, and found the estimated M_3 single hole emission profile to be relatively insensitive to choice of these parameters. In figure 10, *b*'s estimate of the M_3 profile (SXS) so obtained is compared with the results of other deep band experimental probe studies: ion neutralization (INS) by Hagstrum and Becker [53]; x-ray induced photoemission (XPS) by Fadley and Shirley [54]; and ultra-violet induced photoemission (UPS) by Eastman [55]. Note particularly the one to one correspondence of structural features in the main SXS and UPS humps and the general agreement as to width and peak location of all 4 measurements.

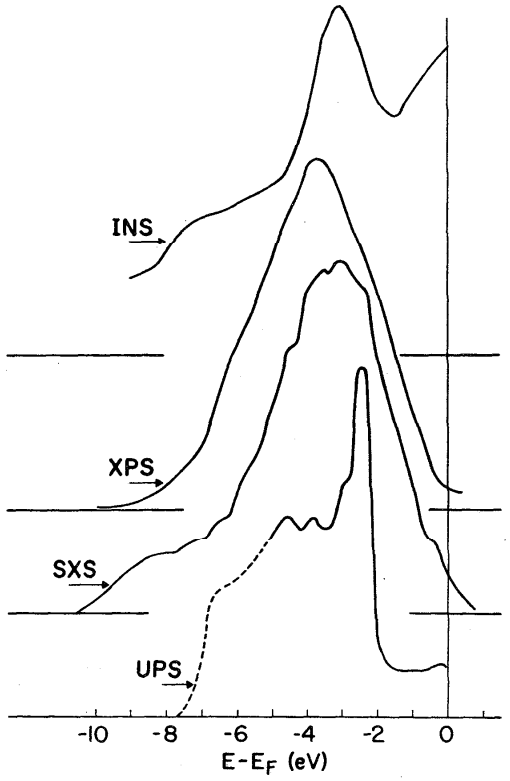

FIGURE 10. Copper.

Comparison of various deep band probe results: ultraviolet photoemission optical density of states (UPS); reduced soft x-ray M_3 emission band (SXS); x-ray photoemission spectrum, with Al $K_{\alpha 1,2}$ excitation (XPS); ion neutralization unfold function (INS).

In figure 11, the lower set of curves compares the experimental M_3 and L_3 single hole emission profiles, the latter determined by Liefeld [24] at threshold excitation. Note particularly the greater width of the M_3 profile in the *d*-hump, and its greater relative intensity below the hump. Qualitatively, these features are predicted in the one-electron transition densities calculated by Goodings and Harris [45], but they are over-ridden in the total emission spectra by the E^3 dependence of the dipole emission rate expression, this factor being important to the M_3 profile only. The Goodings and Harris results for the M_3 and L_3 Cu emission profiles are shown as the middle pair of curves in figure 3, where many-body level broadening has been taken into account with Blokhin and Sachenko's approximation [56] to the Landsberg [7] free electron result. *b* noted that if emission takes place after screening of the inner level defect, one might reasonably expect large positive *s*-wave and small negative *d*-wave shifts in the screening cloud. Thus the *s*-like fraction of the calculated emission spectrum could be enhanced relative to the *d* by a factor in excess of one, and the above mentioned differences in one electron transition rates enhanced by the

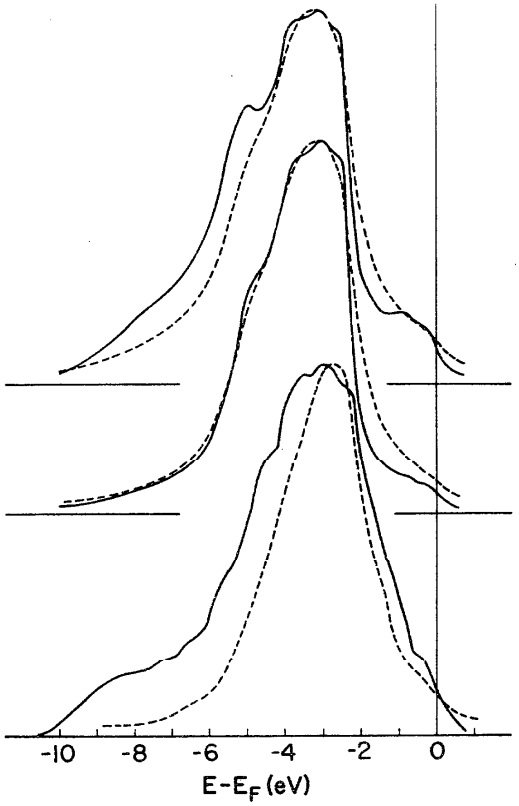

FIGURE 11. Copper.

Comparison of measured and calculated Cu L_3 (dashed) and M_3 (solid) emission spectra. Lower curves, measured. Middle curves, band theory estimate. Upper curves, band theory with approximate screening correction.

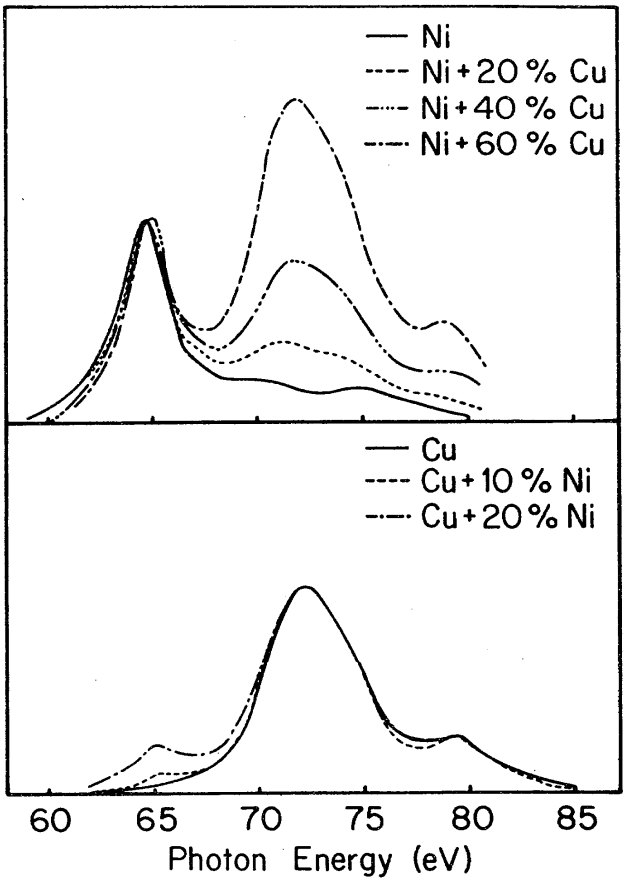

FIGURE 12. Copper and nickel in Cu-Ni.

Soft x-ray $M_{2,3}$ spectra from a number of alloys and the pure metals.

screening. They tested this mechanism in a rough way by assuming various energy independent s to d enhancement factors and then recomputing the spectra. Their results for $s/d=5$ are shown at the top of figure 11. Agreement with experiment was noticeably improved, but no rationalization of the factor used was offered.

Cu and Ni in Cu-Ni

Cu and Ni form a continuous series of solid solutions over the entire composition range, the lattice constant increasing by 2.7 percent from Ni to Cu. It is therefore an attractive system for studying the effects of substitutional disorder on the electronic structure of metals. Homogeneity is difficult to achieve, however, and for this reason some of the results presented here must be regarded with caution. (The question of homogeneity in Cu-Ni alloys has been reviewed by Seib and Spicer [57].) While not enough work has been done to permit intercomparison of soft x-ray results, sufficient other deep band probe studies have been made to warrant their summary. Presented here are: *a*) soft x-ray emission bands (SXS) (Clift, et al. [51]); *b*) x-ray photoemission spectra (XPS) (Hüfner, et al. [58]); *c*) ultraviolet photoemission (UPS) (Seib and Spicer [57, 59]); *d*) soft x-ray L_3 absorption spectra (Van Den Berg [60]).

a gives (SXS) $M_{2,3}$ emission spectra of the pure metals and both components of the alloys, in 10 percent concentration steps across the composition range. No details of sample preparation were given. Some of their results are shown in figure 12, plotted as intensity vs photon energy. The spectra were excited with a 3.5 keV electron beam normally incident on the samples. X-ray takeoff was at 30° from the sample surface. Samples were water cooled. Pressure was approximately 1×10^{-6} torr. Photographic detection was used. The plotted curves were obtained by averaging densitometer traces of several exposures at 0.5 eV intervals, and drawing a smooth curve through the points. Thus, even in the pure metals, detail such as that observed by Cuthill, et al. [22] for pure Ni and Dobbyn, et al. for Cu [21] is eliminated, and no light is shed on the interesting question of its survival or change with alloying.

b's XPS spectra of the valence bands of Cu, Ni, and 12, 44, 46, and 74 percent of Cu in Ni are shown in figure 13. Al $K_{\alpha 12}$ radiation was employed; resolution was approximately 1.0 eV. No details of sample preparation are given. Ar ion cleaning was employed prior to measurements.

The samples upon which *c* performed UPS measurements fall into three classes: 0, 13, and 23 percent Ni in Cu, single crystal, the alloys vacuum annealed at 1000° C for 13 days and air quenched, all three cleaned in vacuum by heating to 600° C; 0, 11, 19, and 49 per-

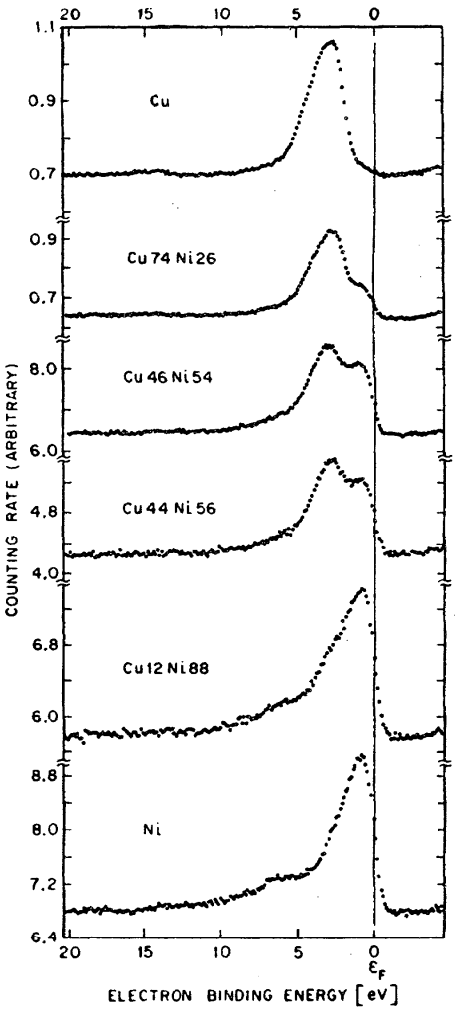

FIGURE 13. Copper and nickel in Cu-Ni.

X-ray photoemission spectra of a number of Cu-Ni alloys.

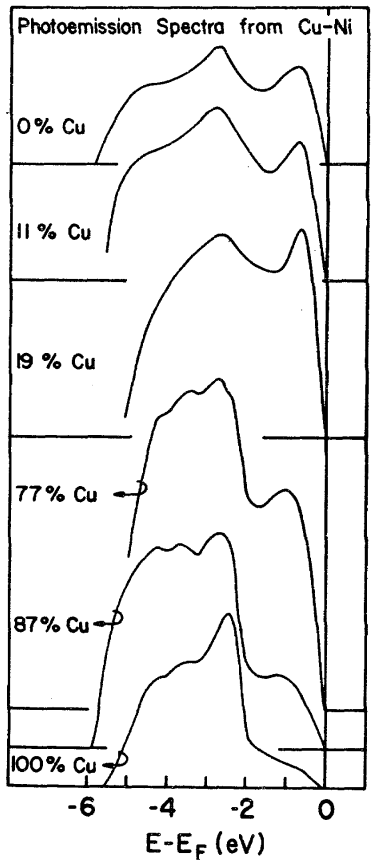

FIGURE 14. Copper and nickel in Cu-Ni.

Ultraviolet photoemission spectra from several Cu-Ni alloys.

cent Cu in Ni, polycrystalline, similarly heat treated, then cleaned in vacuum by successive Ar bombardments followed by 355° C annealing; 39 and 62 percent Cu in Ni, no heat treatment, cleaned in vacuum like the latter. The alloys of 39, 49, and 62 percent Cu in Ni proved unsatisfactory in several respects and will not be discussed here. Figure 14 shows photoemission spectra from samples of 0, 13, and 23 percent Ni in Cu, taken with 10.2 eV photons, and 81, 89, and 100 percent Ni in Cu, taken with 10.0 eV photons. Resolution is about 0.2 eV.

Both *a* and *b* note that to a good approximation, their results can be reproduced by superimposing the pure metal results. *c* on the other hand asserts that the Ni density of states is narrow (~1 eV) at low Ni concentrations, and broadens to about 5 eV for pure Ni. There is reason to doubt the validity of this description at low Ni concentrations, however. *c* bases this assertion largely on an attempt to remove the Cu contribution to the observed spectra at 13 and 23 percent Ni by scaling the pure Cu spectrum to full experimental intensity for the alloys at −2.2 eV and subtracting. The resulting curves

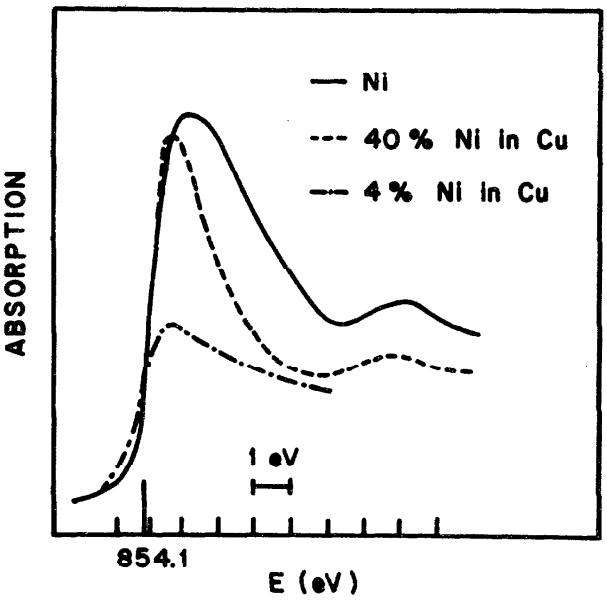

FIGURE 15. Nickel in Cu-Ni.

Soft x-ray L_3 absorption spectra of Ni in pure Ni and two Cu-Ni alloys.

not only show a peak at about −1.0 eV, but an additional peak at −3.0 eV, together with a deep, sharp, obviously spurious minimum at −2.2. Reducing the scale factor for Cu from full to about 0.7 of the experimental intensity at −2.2 largely removes the strange minimum, and leaves an estimated Ni curve quite like that of pure Ni, but with about a −0.2 eV chemical shift. Thus, it would appear that all three techniques can be reasonably construed to yield compatible results.

An additional interesting experimental observation is that of figure 15. Shown here are *d*'s measurements of the soft x-ray L absorption edge of Ni in pure Ni and 4 and 40 percent Ni in Cu. The striking feature here is the persistence of the strong peak at the edge, usually attributed to *d*-holes above the Fermi level. This result is again consistent with those cited above, but the quality of the samples, described only as evaporated films, is open to question.

Finally, Wenger, et al. [61] have attempted to obtain a measure of the *s-d* charge at Ni sites in Cu-Ni alloys by measuring the integrated intensity of the Ni L_α emission band normalized to that of the Ni L_1 line ($3s \rightarrow 2p^{3/2}$) at 20 percent intervals across the series. They found it to be constant within experimental error. No details of sample preparation were given.

Further clarification of the experimental situation is needed, particularly at low Ni concentrations. SXS measurements should be particularly valuable here, because of the partial resolution of the component emission spectra, but optimum resolution, linearity, and signal to noise ratio must be achieved if genuine improvements are to be made.

Li

Figure 16 compares Li K emission profiles recorded by *a*) Crisp and Williams [62], and *b*) Tomboulian and Bedo [6]. These two results are quite representative of the available literature. In each case, measurements were made on samples freshly evaporated in vacuum. Pressures were approximately 10^{-5} torr during evaporation, and 10^{-6} during measurement. (More recent measurements by Aita and Sagawa [63], made under better vacuum, 10^{-7} to 10^{-8} torr, are compatible with these results.) In *a*, electromagnetic detection was used, and ratemeter strip chart records averaged. In *b*, photographic detection was used. Sample temperature was stated by *b* as 162° C; *a* used a watercooled sample, but reported no temperature. In each case, the samples were metallic, and retained bright metallic luster during the measurements. The only significant difference between the two profiles is in the high energy edge, the results of *a* being noticeably sharper there. In this connection, it is worth noting differences in excitation conditions: *a*) electron beam of 4 keV, incident at 90°, x-ray takeoff of ~ 15°; *b*) electron beam of 0.75 keV at 90°, x-ray takeoff of 45°. The sharper edge of *a* appears to be a self-absorption artifact.

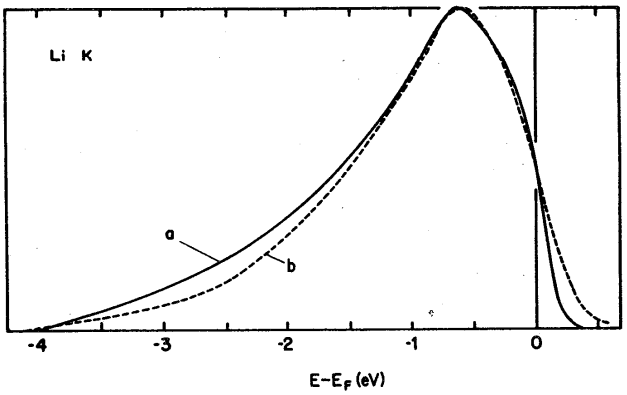

FIGURE 16. Lithium.

Two measured soft x-ray Li K emission profiles.

The pre-peaking of the Li K emission spectrum (maximum intensity occurs 0.6 eV below the Fermi edge, rather than at the edge as predicted by one-electron theory) has not as yet received definitive explanation. It is certain that no band calculation based on Hartree-Fock type orbitals and using conventionally constructed crystal potentials will yield an early peak (McAlister [64]). However, the new band calculation approach of Goddard (see O'Keefe and Goddard [65]). using spin generalized rather than Hartree-Fock basis orbitals, does offer a band structure explanation. Since the removal of a core electron from Li constitutes an extremely large perturbation, screening effects have been plausibly invoked (Goodings [4]; Allotey [5]; Ausman and Glick [66]). None of these approaches offers any explanation of the extreme overlap of the emission and absorption edges (Skinner and Johnston [67]), and their Gaussian tails. McAlister [64] has shown that folding one electron estimates of the emission and absorption rates with a broad Gaussian smearing function yields good agreement with experiment. He attributes the Gaussian smear to thermal broadening of the K level by the phonon field, but offers no rationalization of the large width (0.3 to 0.4 eV) needed for a good fit.

Mg

Numerous measurements have been made of the Mg $L_{2,3}$ emission spectrum, all showing a rather sharp peak just below the high energy emission edge. The three measurements of figure 17 are due to *a*) Watson, et al. [68]; *b*) Neddermeyer [27]; and *c*) Fomichev [69]. In no case were temperatures stated, but watercooled cathodes were used by *a* and *c*. Electron beam excitation was used in each case: *a*, 3.0 keV; *b*, 2.0 keV; *c*, not stated. None cite x-ray takeoff or electron impingement angles. Pressures cited were *a*, 1×10^{-6} torr; *b*, $1 - 3 \times 10^{-8}$ torr; *c* not stated. All used blazed metal coated gratings, *a* and *c* Au coated, *b* Pt coated. Photoelectric detection was used in each case. *a* summed digitally recorded runs; *b* summed strip chart recorded scans; *c* used a single, stepped counting sweep. Neither *b* or *c* cite noise figures for their data. *a* plotted data

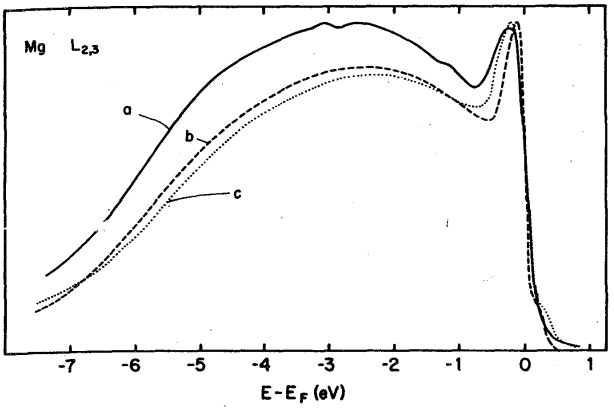

FIGURE 17. Magnesium.

Three measured Mg $L_{2,3}$ soft x-ray emission profiles.

with vertical bars representing the standard counting error, $\pm\sqrt{N}$, N being the total number of counts per channel. Their statistical noise level was sufficiently low that the small features at -1.3 and -2.9 eV appear real. Independent, unpublished measurements of Dimond displayed by *a*, show like structure. An approximate theoretical analysis, similar to that by Rooke for Al [32] was carried out by *a*. The analysis suggests a one electron interpretation for the minimum at about -0.8 eV on their curve, and the feature at -1.3 eV. The analysis suggests no explanation for that at -2.9. The calculated positions for the minimum and slope break are -0.9 and -1.7 eV, respectively. The feature at -2.9 remains unexplained. *a* suggests the possibility that it is an oxide structure. However, it shows no correlation with the Mg spectrum from bulk MgO (Neddermeyer [28], Formichev, et al. [70]).

Mg in Al-Mg

See Al and Mg in Al-Mg.

Na

The measurements of the Na $L_{2,3}$ profile shown in figure 18 are due to *a*) Crisp and Williams [62]; *b*) Skinner [9], and *c*) Cady and Tomboulian [39]. *a*) used photoelectric detection, and averaged several strip chart records. Rooke [71] has produced a sum of digitally recorded scans, made on the same instrument and in essential agreement with *a*. *b* used photographic recordings. A photographic measurement by Sen [72] agrees well with *b*. *c* used photographic detection. All reported measurements were carried out at 1 to 5×10^{-6} torr. Sample surface cleanliness is suspect at such high pressures, but Na at least retains its metallic luster during the course of the measurements. Temperatures were uncertain, but all measurements were made on the solid. The sharp pip at the emission edge seen in *a* and *b* (and by Rooke [71] and Sen [72] as well) is surely characteristic of measurements made at high excitation voltage and unfavorable excitation geometry. *c* took experimental precautions at least as extensive as the other workers. Their measurements of the Al and Mg $L_{2,3}$

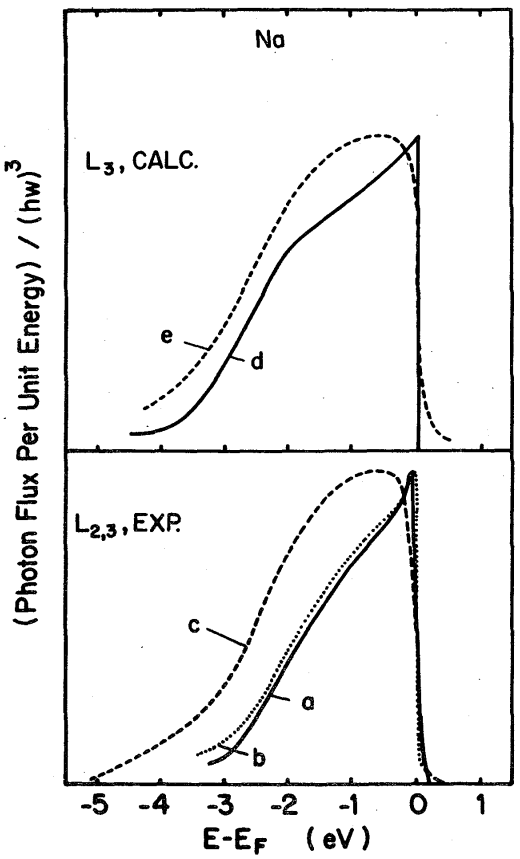

FIGURE 18. Sodium.

Measured $L_{2,3}$ soft x-ray profiles, *a*–*c*. Band theory estimate of the profile, *e*; many body theory profile estimate, *d*.

profiles reported at the same time are in line with other experimental results. However they report an r.m.s. electron beam exciting voltage of 1.4 keV, while that of other workers ranges from 3.5 to 4-0 keV. Additionally, Haensel, et al. [73] have reported a measurement of the Na $L_{2,3}$ absorption profile which shows a distinct minimum approximately 0.2 eV below the mid-point of the L_3 edge. The pip in *a* and *b* occurs approximately 0.15 eV below the 50 percent point of the emission edge. Unfortunately, the absorption data extend only 0.6 eV below the mid-point of the edge, and only the shape of the absorption edge, not its absolute magnitude, is reported. These factors suggest that the edge pip may be a self absorption artifact. Further experimental work is needed to clarify this point.

The importance of answering this question is emphasized by the two theoretical estimates shown in the upper part of the figure. *d* is the result of a many body calculation by Glick, et al. [13]. It includes in a natural way the effects of the core hole and final state interactions, and shows a distinct rise in intensity just at the Fermi edge. *e* is a band theory estimate by McAlister [74], with level broadening treated in the Landsberg approximation [7]. It would agree fairly well with experimental curve *c* if some degree of energy dependent enhancement by core hole screening were assumed.

Ni

The L_3 emission profile of Ni has been studied by many investigators (Farineau [47], Skinner, et al. [75], Cauchois [76], for example), with considerable disagreement in the results. Van Den Berg [60] made the first progress in solving the problem by noting that the measured profile depended strongly on the energy of the exciting electron beam. More recently, Bonnelle [23] and, particularly, Liefeld and co-workers [24, 25] have shown the disparities to arise from the fact that satellite intensity and self absorption effects can be very important and depend markedly on exciting electron beam energy. In figure 19 are shown results of Liefeld [24] and Chopra [77] on the L_3 profile of Ni. Measurements were made at a sample temperature of about 800° C, at approximately 1×10^{-7} torr in a 2 crystal instrument. Various exciting electron beam voltages, V_x, were used. Curve *a* is typical of results with V_x between the L_3 and L_2 threshold. For V_x above the L_2 threshold, holes can be created in the $2p^{1/2}$ core shell, and the Auger decay $2p^{1/2} \rightarrow (2p^{3/2}, v)$, where v denotes a hole in the valence band, can occur. Radiative decay can then occur with a local, relatively high mass spectator hole in a $3d$ level, and high energy satellite structure appears, as in curve *b*. As one continues to raise V_x, the satellite structure increases in intensity, as in *c*. Eventually, as in curves *d*, and *e*, self absorption becomes sufficiently strong to warp the measured profiles in a pronounced way. In fact, the L_3 absorption spectrum can be obtained by taking the ratio of profiles measured at two suitable values of V_x (Liefeld [24]). Bonnelle [23] independently demonstrated the dependence of self absorption on V_x, and in addition, showed how it can be reduced by optimizing x-ray takeoff and exciting electron beam incidence angles.

Various measurements on the Ni $M_{2,3}$ spectrum (Tomboulian and Bedo [78], Skinner, et al. [75], Clift, et al. [51], Cuthill, et al. [22]) have shown better agreement, the situation being comparable to that shown above for the $M_{2,3}$ spectra of Cu. There are several probable causes for this. The $M_{2,3}$ measurements were made over a less extreme range of V_x, 2.5 to 4.0 keV. Too, as noted above for Cu, the M-valence band satellites tend to be degenerate in energy with the M_2 band. And finally, self absorption should be much less severe, owing to the very broad and only softly structured $M_{2,3}$ absorption edges (Sonntag [79]).

In figure 20, a number of deep band electronic structure probe results on Ni are compared: the M_3 profile of Cuthill, et al. [22], extracted from the $M_{2,3}$ complex in the manner described above for Cu; the L_3 profile, measured at L_3 threshold excitation by Liefeld [24]; the XPS spectrum of Fadley and Shirley [54]; the ultraviolet induced photoemission optical density of states of Eastman and Krolikowski [80]; and the ion neutralization unfold function of Hagstrum and Becker

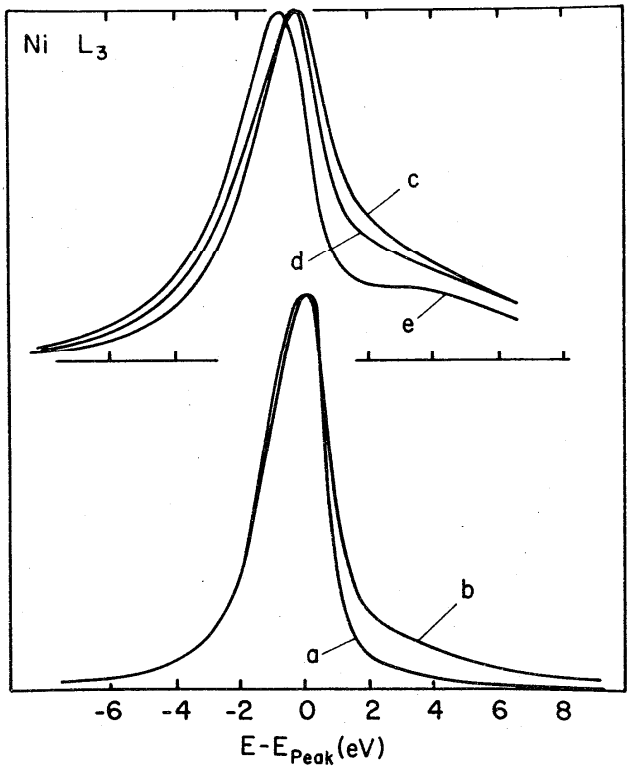

FIGURE 19. Nickel.

The Ni soft x-ray L_3 profile, measured at a number of exciting electron beam energies. The voltages are, in keV: *a*) 0.86, *b*) 0.92, *c*) 2.0, *d*) 5.1, *e*) 12.5.

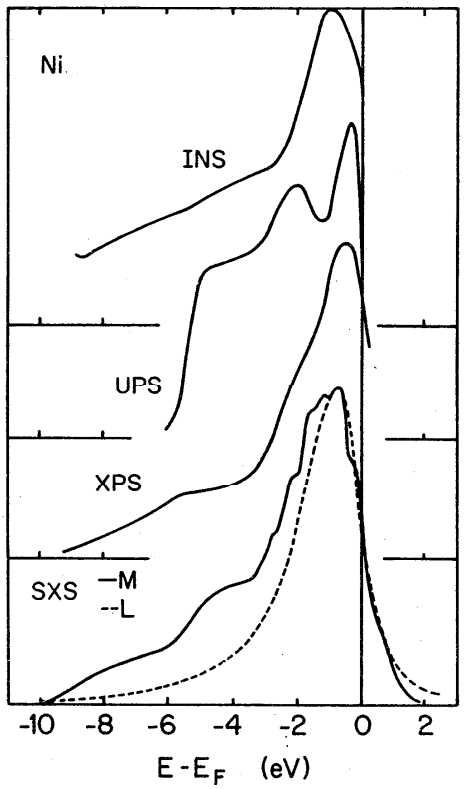

FIGURE 20. Comparison of various deep band probe results for Ni.

Lowest curves, soft x-ray L (dashed) and M (solid) emission spectra (SXS). X-ray photoemission spectrum (XPS); ultraviolet photoemission optical density of states (UPS); ion neutralization unfold function (INS).

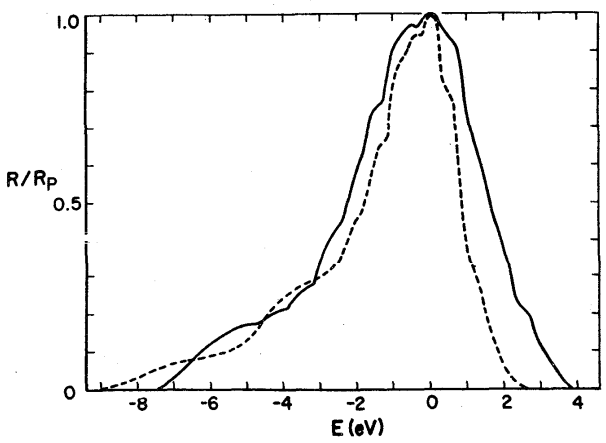

FIGURE 21. Nickel and copper.

Comparison of Ni (dashed) and Cu (solid) $M_{2,3}$ emission bands, showing structural correlation.

[53]. Here, as in the case of Cu discussed above, remarkably strong structural correlations are observed, despite differences in magnetic state. The soft x ray measurements were made on paramagnetic Ni (at 960°C for the M, 800°C for the L) while the photoemission and ion neutralization measurements were made at room temperature on ferromagnetic samples. Figure 21 compares the M_3 profiles of Cu (Dobbyn, et al. [21]) and paramagnetic Ni (Cuthill, et al. [22]). Structural correlation between the two spectra is evident, and to be expected from their common crystal structure and valence difference of 1. Note however the slight shoulder on the high energy side of the "*d*-hump" in both spectra. Similar structure has been noted by the present authors in unpublished measurements of the M spectra of Cr and Fe. Liefeld and Hanzely [25] also report like structure in their threshold measurements of the L_3 spectra of Cu, Ni, Co, and Fe. These have been plausibly interpreted as excitation features (Dobbyn [21], Liefeld [25]) of the type described by Parratt [17].

Ni in Cu-Ni

See Cu and Ni in Cu-Ni

References

[1] W. V. Houston, Phys. Rev. **38**, 1791 (1931).
[2] H. Jones, N. F. Mott, and H. W. B. Skinner, Phys. Rev. **45**, 379 (1934).
[3] J. Friedel, Phil Mag. **43**, 153 (1952).
[4] D. A. Goodings, Proc. Phys. Soc. (London) **86**, 75 (1965).
[5] F. K. Allotey, Phys. Rev. **157**, 467 (1967).
[6] D. H. Tomboulian and D. E. Bedo, Phys. Rev. **109**, 35 (1958).
[7] P. T. Landsberg, Proc. Phys. Soc. (London) **A62**, 806 (1949).
[8] G. A. Rooke, Physics Letters **3**, 234 (1963).
[9] H. W. B. Skinner, Phil. Trans. Roy. Soc. (London) **239A**, 95 (1940).
[10] D. Bohm and D. Pines, Phys. Rev. **92**, 609 (1953).
[11] J. Pirenne and P. Longe, Physica **30**, 277 (1964).
[12] A. J. Glick and P. Longe, Phys. Rev. Letters **15**, 589 (1965).
[13] A. J. Glick, P. Longe, and S. M. Bose, in *Soft X-Ray Band Spectra*, edited by D. J. Fabian (Academic Press, New York, 1968), p. 319.
[14] G. D. Mahan, Phys. Rev. **163**, 612 (1967).
[15] P. Nozieres and C. T. de Dominicis, Phys. Rev. **178**, 1097 (1969).
[16] L. Hedin and S. Lundqvist in *Solid State Physics, Volume 23* edited by F. Seitz, D. Turnbull, and H. Ehrenreich (Academic Press, New York, 1969) page 1.
[17] L. G. Parratt, Rev. Mod. Phys. **31**, 616 (1959).
[18] *Soft X-Ray Band Spectra*, edited by D. J. Fabian (Academic Press, New York, 1968).
[19] J. A. R. Samson, *Techniques of Vacuum Ultraviolet Spectroscopy* (John Wiley and Sons, New York, 1967).
[20] H. Neddermeyer and G. Wiech, Physics Letters **31A**, 17 (1970).
[21] R. C. Dobbyn, M. L. Williams, J. R. Cuthill, and A. J. McAlister, Phys. Rev. **B2**, 1563 (1970).
[22] J. R. Cuthill, A. J. McAlister, M. L. Williams, and R. E. Watson, Phys. Rev. **164**, 1006 (1967).
[23] C. Bonnelle, Ph.D. Thesis, U. of Paris, 1964, unpublished.
[24] R. J. Liefeld, in *Soft X-Ray Band Spectra*, edited by D. J. Fabian (Academic Press, New York, 1968), p. 133.
[25] S. Hanzely and R. J. Liefeld, in *Electronic Density of States* edited by L. H. Bennett, Nat. Bur. Stand. (U.S.) Spec. Pub. 323, 1971, page 319.
[26] H. Yakowitz and K. F. J. Heinrich, Mikrochim. Acta, 182 (1968).
[27] H. Neddermeyer, in *Electronic Density of States*, edited by L. H. Bennett, Nat. Bur. Stand. (U.S.), Spec. Pub. 323, 1971, page 313.
[28] H. Neddermeyer, Ph.D. Thesis, Ludwig Maximillian University, 1969, unpublished.
[29] F. Wooten, T. Huen, and R. Stewart, in *Optical Properties of Metals and Alloys*, edited by F. A. Abeles, (North-Holland, Ambsterdam, 1966) page 333.
[30] V. A. Fomichev, Soviet Physics-Solid State **8**, 2312 (1967).
[31] G. A. Rooke, J. Phys. C **1**, 776 (1968).
[32] G. A. Rooke, J. Phys. C **1**, 767 (1968).
[33] L. Smrcka, Czech. J. Phys. **B21**, 683 (1971).
[34] A. J. McAlister, unpublished.
[35] T. Sagawa, in *Soft X-Ray Band Spectra*, edited by D. J. Fabian (Academic Press, New York, 1968), p. 29.
[36] A. Appleton and C. Curry, Phil Mag. **12**, 245 (1965).
[37] R. K. Dimond, Phil Mag. **15**, 631 (1967).
[38] J. A. Catterall and J. Trotter, Phil Mag. **8**, 897 (1963).
[39] W. M. Cady and D. H. Tomboulian, Phys. Rev. **59**, 381 (1941).
[40] R. D. Deslattes, private communication. The curve shown was obtained by averaging two raw spectra, kindly supplied by Dr. Deslattes, and subtracting a constant background correction.
[41] C. Sénémaud, Ph.D. Thesis, U. of Paris, 1968, unpublished. This result is reproduced by Y. Cauchois in *Soft X-Ray Band Spectra*, edited by D. J. Fabian (Academic Press, New York, 1968) page 71. The present data is a revision of earlier work by these authors, J. Phys. Radium **27C2**, 55 (1966).
[42] M. L. Williams, R. C. Dobbyn, J. R. Cuthill, and A. J. McAlister in *Electronic Density of States*, edited by L. H. Bennett, Nat. Bur. Stand. (U.S.) Spec. Pub. 323, 1971, page 303.
[43] C. Curry and R. Harrison, Phil. Mag. **21**, 659 (1970).
[44] A. C. Switendick in *Electronic Density of States*, edited by L. H. Bennett, Nat. Bur. Stand. (U.S.) Spec. Pub. 323, 1971, page 297.
[45] D. A. Goodings and R. Harris, J. Phys. C. **2**, 1808 (1969).
[46] L. H. Bennett, A. J. McAlister, J. R. Cuthill, and R. C. Dobbyn in *Electronic Density of States*, edited by L. H. Bennett, Nat. But. Stand. (U.S.) Spec. Pub. 323, 1971, page 665.
[47] J. Farineau, Annales de Physique **10**, 20 (1938).
[48] D. W. Fischer and W. L. Baun, Advances in X-Ray Analysis **10**, 374 (1967).
[49] R. L. Jacobs, Physics Letters **30A**, 523 (1969).
[50] D. E. Bedo and D. H. Tomboulian, Phys. Rev. **113**, 464 (1959).
[51] J. Clift, C. Curry, and B. J. Thompson, Phil Mag. **8**, 593 (1963).
[52] S. Roberts, Phys. Rev. **118**, 1509 (1960).
[53] H. D. Hagstrum and G. E. Becker, Phys. Rev. **159**, 572 (1967).
[54] C. S. Fadley and D. A. Shirley, Phys. Rev. Letters **21**, 980 (1968).

[55] D. E. Eastman, J. Appl. Phys. **40**, 1387 (1969).
[56] M. A. Blokhin and V. P. Sachenko, Bull. Acad. Sci., USSR, Phys. Ser. **24**, 10 (1960).
[57] D. H. Seib and W. E. Spicer, Phys. Rev. B **2**, 1676 (1970).
[58] S. Hüfner, G. K. Wertheim, R. L. Cohen, and J. H. Wernick, Phys. Rev. Letters **28**, 488 (1972).
[59] D. H. Seib and W. E. Spicer, Phys. Rev. B **2**, 1694 (1970).
[60] C. B. Van Den Berg, Ph.D. Thesis, U. of Groningen, 1957, unpublished.
[61] A. Wenger, G. Burri, and S. Steinemann, Phys. Letters **34A**, 195 (1971).
[62] R. S. Crisp and S. E. Williams, Phil Mag. **6**, 365 (1961); see also R. S. Crisp, Ph.D. Thesis, U. of Western Australia, 1961, unpublished.
[63] O. Aita and T. Sagawa, J. Phys. Soc. Japan **27**, 164 (1969).
[64] A. J. McAlister, Phys. Rev. **186**, 595 (1969).
[65] P. M. O'Keefe and W. A. Goddard, Phys. Rev. Letters **23**, 300 (1969).
[66] G. A. Ausman and A. J. Glick, Phys. Rev. **183**, 687 (1969).
[67] H. W. B. Skinner and J. E. Johnston, Proc. Roy. Soc. (London) **161A**, 420 (1937).
[68] L. M. Watson, R. K. Dimond, and D. J. Fabian, in *Soft X-Ray Band Spectra*, edited by D. J. Fabian (Academic Press, New York, 1968) page 45.
[69] V. A. Fomichev, T. M. Zimkina, and I. I. Zhukova, Soviet Physics-Solid State **10**, 2992 (1969).
[70] V. A. Fomichev, T. M. Zimkina, and I. I. Zhukova, Soviet Physics-Solid State **10**, 2421 (1969).
[71] G. A. Rooke in *Soft X-Ray Band Spectra*, edited by D. J. Fabian (Academic Press, New York, 1968), p. 3.
[72] A. Sen, Indian J. Phys. **30**, 415 (1956).
[73] R. Haensel, G. Keitel, P. Schreiber, B. Sonntag, and C. Kunz, Phys. Rev. Letters **23**, 528 (1969).
[74] A. J. McAlister, unpublished.
[75] H. W. B. Skinner, T. G. Bullen, and J. E. Johnston, Phil. Mag. **45**, 1070 (1954).
[76] Y. Cauchois, Phil. Mag. **44**, 173 (1953).
[77] D. R. Chopra, Ph.D. Thesis, New Mexico State University, 1964, unpublished.
[78] D. H. Tomboulian and D. E. Bedo, Phys. Rev. **121**, 146 (1961).
[79] B. Sonntag, Deutches Elektronen Synchrotron, Hamburg, Internal Report DESY-F41/1, 1969, unpublished.
[80] D. E. Eastman and W. F. Krolikowski, Phys. Rev. Letters **21**, 623 (1968).